

Temperature Dependence of Structure and Dynamic Properties of Oleic Acid γ and α Phases Studied by FTIR Spectroscopy

Fuwei Pi,[1] Fumitoshi Kaneko,*[2] Hideyuki Shinzawa,[3] Masao Suzuki,[4] Makio Iwahashi,[5] and Yukihiro Ozaki*[1]

[1]Department of Chemistry, School of Science and Technology, Kwansei Gakuin University, Sanda, Hyogo 669-1337

[2]Department of Macromolecular Science, Graduate School of Science, Osaka University, Toyonaka, Osaka 560-0043

[3]Advanced Industrial Science and Technology (AIST), Nagoya, Aichi 463-8560

[4]Research Institute of Biological Materials, Keihanna Research Laboratories, 1-7 Hikaridai, Seika, Soraku-gun, Kyoto 619-0237

[5]Department of Chemistry, School of Science, Kitasato University, 1-15-1 Kitasato, Minami-ku, Sagamihara, Kanagawa 252-0373

Received November 11, 2010; E-mail: ozaki@kwansei.ac.jp, toshi@chem.sci.osaka-u.ac.jp

The temperature dependence of the structure and dynamic properties of oleic acid γ and α phases has been studied by FTIR spectroscopy. By observing the characteristic bands due to the *cis*-olefin, carboxy, and methyl groups as well as the CH_2 rocking–CH_2 twisting progression bands, the structural change of each portion of oleic acid corresponding to the $\gamma \rightarrow \alpha$ phase transition has been elucidated in detail. For the analysis of the progression bands, the simple-coupled oscillator model has been employed. It has been found that an enhanced mobility of the methyl terminal occurs as the temperature increases in the γ phase, which operates as pre-disordering prior to the sudden and drastic structural changes at the $\gamma \rightarrow \alpha$ phase-transition point. Meanwhile, the carboxy group undergoes a gradual and localized structural change in the γ phase. The structural change of carboxy group in the γ phase is likely to be caused by an equilibrium shift between two different states of dimerized carboxy groups. Drastic structural changes at the phase-transition point primarily take place in the portion from the *cis*-olefin group to the methyl group, which is fully consistent with previous studies by X-ray and Raman spectroscopy. It is clearly shown that the CH_2 rocking–CH_2 twisting progression bands can be employed as a probe for sensing the states of the methyl-sided and carboxy-sided chains separately, which is applicable for the structural studies of a wide range of fats and lipids systems containing unsaturated acyl chains.

cis-Unsaturated fatty acids are major building blocks of most natural lipids such as phospholipids and glycolipids and widely distributed in biological tissues.[1,2] The amounts and types of *cis*-unsaturated fatty acids contained in phospholipids have a great influence on the functional activities of biological membranes.[3,4] It is well known that *cis*-unsaturated acyl chains, which are mostly linked to the second position of phospholipids, disturb stable close-packed structures of acyl chains because of the large steric hindrance due to the bent *cis*-olefinic conformation, thereby keeping the mobility and permeability of biological membranes even at low temperatures.[2,5] It has also been reported that lipid compounds with one *cis*-unsaturated acyl chain tend to exhibit a variety of aggregation states due to flexible conformation.[6–8] Research on the polymorphism and phase-transition behavior of *cis*-unsaturated fatty acids would provide concrete information about the structure and properties of *cis*-unsaturated acyl chains in aggregation states, such as favorable lateral packing of hydrocarbon chains, conformational variety of *cis*-olefin groups, and mobility of each part, which would be fundamental knowledge for studies on more complex systems that include unsaturated acyl chains.

Oleic acid (*cis*-9-octadecenoic acid), which is the most abundant *cis*-monounsaturated fatty acid in nature, has been attracting considerable attention from various fields of science and technology.[1,2] The schematic structure and functional sections of oleic acid are illustrated in Figure 1a. The use of oleic acid and its derivatives has become of importance in the pharmaceutical, food, and cosmetic industries.[9] It has three polymorphic phases, α (mp 13.3 °C), β (mp 16.2 °C), and γ.[10–12] The crystal structures of the γ and β phases have already been determined by X-ray crystallography.[13,14] Moreover, based on Raman spectral measurements, the γ phase is assumed to undergo a first-order solid-state reversible transition with a selective conformational disordering in the methyl-terminus hydrocarbon chain to the α phase at -2.2 °C on heating.[15,16] Detailed structural and thermodynamic information about the γ, α, and β phases is given in the Background section following this introduction. The α and γ phases have been found in other *cis*-monounsaturated fatty acids, palmitoleic acid, erucic acid, gondoic acid, and asclepic acid,[12,17–20] whereas the β phase has been found only in oleic acid.

The conformational disordering of the methyl-terminus chain of the $\gamma \rightarrow \alpha$ reversible solid-state phase transition can be

Published on the web April 7, 2011; doi:10.1246/bcsj.20100314

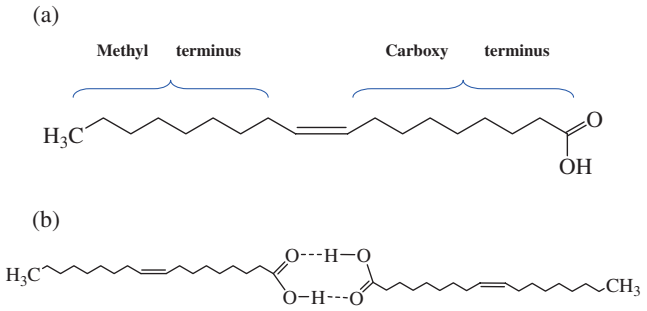

Figure 1. Schematic drawings: (a) oleic acid molecule and (b) dimerized oleic acid molecules.

regarded as a characteristic of *cis*-monounsaturated acyl chains. Such partial melting at lamellar interfaces has not been found in other long-chain compounds consisting of saturated acyl chains.[15] Therefore, detailed information about the transition mechanism is essential for understanding the influence of *cis*-unsaturation on aggregation states of fats and lipids in biological tissues. Structures of the γ and α phases have been studied by X-ray crystallography,[13] vibrational spectroscopy,[15,16,21] and NMR spectroscopy,[22] which has shown large structural and dynamic differences in the portion from the *cis*-olefin group to the methyl terminus between the two solid phases. Nevertheless, until now the temperature-dependent conformational change of oleic acid has been mainly followed by Raman spectroscopy. Kobayashi et al. pointed out that the selective conformational disordering takes place in the methyl-terminus chain in the α phase based on the spectral changes in the C–C stretching region.[15] The validity of this proposition was studied by Kim et al. and Tandon et al. through observing the Raman bands due to methyl rocking, C–C stretching, and other modes.[16,21] The Raman data clarified that the conformational disordering starts suddenly at the transition point. However, so far, there has been no detailed FTIR spectroscopic study that deals with the temperature-dependent structural changes and dynamic properties of the γ to α phase transition.

FTIR spectroscopy provides a full IR spectrum in a short time, which allows us to get a variety of structural information at once, and can provide complementary information with that of Raman spectroscopy: it is susceptible to the structural changes of polar groups such as carboxy and methyl groups. Therefore, it would shed some light on the behavior of the carboxy and methyl groups in the γ and α phases that has not drawn much attention to up to now. Furthermore, a few series of bands associated with hydrocarbon chains called progression bands appear in FTIR spectra; these bands can possibly be used as a new probe for sensing the local structure of oleoyl groups.

In the present study, by observing the characteristic bands due to the *cis*-olefin, carboxy, and methyl groups as well as the CH_2 rocking–CH_2 twisting progression bands, we tried to follow the temperature-dependent structural changes in the γ and α phases. For this purpose, we analyzed the assignment of the CH_2 rocking–CH_2 twisting progression bands with the simple coupled oscillator model and succeeded to assign most of the progression bands. The first half of the Results section is devoted to this analysis and the second half is devoted to the spectral changes of the progression bands together with those of other characteristic bands. The temperature dependences of these bands provided valuable information about the condition of each hydrocarbon chain at both sides of the *cis*-olefin group. Furthermore, we employed numerical analysis of FTIR spectroscopy such as the second derivative.

It has been found that the structural changes of oleic acid at different parts in the $\gamma \rightarrow \alpha$ phase transition fall into two major categories. One is the sudden and drastic changes at the phase-transition point, and the other is the continuous evolutions in the γ phase. On the basis of the spectral changes obtained in this study as well as the structural information of the previous studies, we will describe the characteristics of the structural changes in each category with the information derived from the spectral changes of the progression bands in detail in the Discussion section. It will be shown that FTIR spectroscopy can be employed as a versatile tool for structural studies on a wide range of fats and lipids systems containing unsaturated acyl chains by combining the analytical methods developed for the spectral data of long-chain compounds.

Background. The crystalline states of oleic acid can be divided into three main states, α, β, and γ, among which the β phase is thermodynamically stable. There is a first-order solid-state phase transition between the α and γ phases. The α phase can be obtained simply by cooling the melt, and on further cooling the α phase transforms into the γ phase around $-4\,^{\circ}C$ reversibly. On heating process, the γ phase changes into the α phase around $-2\,^{\circ}C$ with a sharp endotherm of $8.8\,kJ\,mol^{-1}$, and the α phase fuses at $13.3\,^{\circ}C$ with an endotherm of $39.6\,kJ\,mol^{-1}$. On the other hand, the β phase is rather difficult to crystallize, because of its very low crystal growth rate. In practice, the β phase is obtainable only by well-controlled crystallization from a melt or a solution. The β phase can be further divided into β_1 and β_2 of slightly different melting points, 16.3 and $16.0\,^{\circ}C$,[14] and the fusion of β_1 is accompanied by an endotherm of $51.9\,kJ\,mol^{-1}$. The β_2 phase is considered to be a kind of transient state to the β_1 phase.

The crystal structure of the γ phase of oleic acid was determined by Abrahamsson and Ryderstedt-Nahringbauer.[13] The unit cell belongs to a pseudo-orthorhombic system of space group, $P2_1/a$, and contains two hydrogen-bonded dimers (Figure 1b) which are related to each other by the symmetry of twofold screw axis (parallel to the b axis) or glide plane (normal to the b axis). The internal rotation angles of two C–C bonds linked to the *cis*-C=C bond are $+133$ and $-133°$, which can be recognized as skew and skew′, respectively. With this conformation, two all-*trans* hydrocarbon chains on both sides of *cis*-C=C bond form an $O'_{\parallel}$ subcell where all the skeletal planes are parallel to each other.

The structure of the α phase was determined in erucic acid.[18] Its unit cell also belongs to a monoclinic system, $P2_1/a$, and contains two hydrogen-bonded dimers. However, the internal rotation angles of two C–C bonds liked to *cis*-C=C bond are $+105$ (carboxy side) and $-173°$ (methyl side), which can be recognized as skew and *trans*, respectively. The carboxy-sided polymethylene chains adopt the $O'_{\parallel}$ subcell as that in the γ phase, but the methyl-sided chains form a looser subcell similar to the $O_{\perp}$ subcell.

The structural analysis of β_1 showed that its unit cell belongs to a triclinic system, $P\bar{1}$, whose asymmetric unit is composed of two independent dimerized molecules, A and B. The β_1 phase forms a unique interdigitated structure, in which the methyl group of molecule A is located on the same plane with the carboxy group of molecule B (vice versa). For the structure around the *cis*-C=C section, both molecules show nearly the same conformation which approximates to *trans–cis–trans* configuration.

Experimental

Materials. Ultrapure oleic acid, whose purity was guaranteed to be more than 99.9%, was supplied by Research Institute of Biological Materials (Kyoto, Japan), and was used without further purification.

Fourier Transform Infrared Spectroscopy. Temperature-dependent FTIR spectra of oleic acid were obtained with a Thermo Nicolet Nexus 470 Fourier transform spectrometer equipped with a MCT detector. Normal transmission IR measurements were carried out with co-adding 128 scans at a 1 cm^{-1} resolution.

To obtain a sample of the γ phase, a drop of liquid oleic acid was sandwiched between a pair of KBr plates, mounted on the cold finger of a cryostat set in the sample compartment of the FTIR spectrometer, and cooled at a rate of 2 °C min^{-1} to −40 °C by pumping liquid nitrogen to the cryostat. The cooled specimen was kept at −40 °C for one hour, and the sample temperature was raised at a rate of 2 °C min^{-1} to a predetermined temperature for measurement and kept for 10 min before IR measurement to ensure the thermal equilibrium between the sample and the cryostat. The sample temperature was monitored by a thermoelectric device with an accuracy of ±0.1 °C. The temperature dependence of FTIR spectra in the whole frequency range is reproduced in Figure 2.

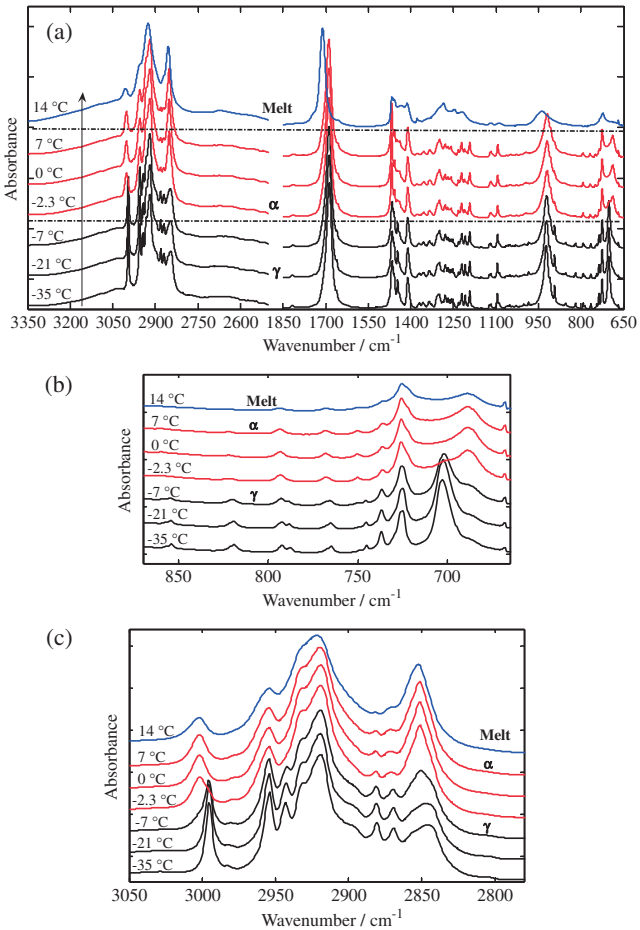

Figure 2. Temperature-dependent FTIR spectra of oleic acid at several selected temperatures: (a) the region of 3350–650 cm^{-1}, (b) an enlargement of the region of 870–650 cm^{-1}, and (c) an enlargement of the region of 3050–2750 cm^{-1}.

Results

Spectral Features of the γ Phase. The hydrocarbon segments of lipid-related compounds exhibit a series of bands called progression bands in IR spectra,[23–28] which are often used as an indicator to monitor the conformational regularity of hydrocarbon chains.[29,30] The IR spectra of the γ phase of oleic acid are rather complex in comparison with the IR spectra of saturated fatty acids.[15,24–26] This is probably caused by the overlapping of the bands of the methyl-terminus chain over those of the carboxy-terminus chain in the same frequency region. Nevertheless, the FTIR spectrum in the 870–715 cm^{-1} region (Figure 3a), where the progression bands due to CH_2 twisting–CH_2 rocking modes (ν_8 branch modes) appear, is relatively simpler than that in the other frequency regions of the γ phase.

According to previous studies on polyethylene[31,32] and *n*-alkanes,[33] the frequency of the ν_8 branch remarkably depends on the phase angle δ (the difference in phase between neighboring CH_2 groups), e.g., the CH_2 rocking mode for $\delta = 0$ appears at 720 cm^{-1} and the CH_2 twisting mode for $\delta = \pi$ appears at 1050 cm^{-1}. Thus, the bands appearing in the 900–700 cm^{-1} region correspond to $\delta = 0$ to 0.7π. Both the methyl-terminus and carboxy-terminus chains consist of the same number of CH_2 groups for oleic acid molecules, but they are different in the boundary conditions (Figure 1a), which has a significant influence on the allowed phase angles, δ_k, of hydrocarbon chains. For the methyl-terminus chain, one end is free and the other end is fixed, whereas both ends of the carboxy-terminus chain are fixed because of dimerized carboxy groups (Figure 1b). When these boundary conditions are applied to the simple-coupled oscillator model, the allowed phase angles can be given by:

$$\delta_k = k\pi/(N+1) \quad k = 1, 2, \ldots, N \tag{1}$$

for the carboxy-terminus chain containing N pieces of CH_2 groups, and

$$\delta_k = (2k-1)\pi/2N \quad k = 1, 2, \ldots, N \tag{2}$$

for the methyl-terminus chain.[15]

Therefore, in spite of the same number ($N = 7$) of CH_2 groups, the allowed δ_k values are different between the methyl-terminus and carboxy-terminus chains. For example, the band around 725 cm^{-1} exhibits an asymmetric profile and its second derivative shows that this band consists at least of three components at 730, 727, and 724 cm^{-1} as shown in Figure 3b, which are attributable to the ν_8 branch modes with $k = 1$ and 2. This overlapping comes from the small dispersions of the ν_8 branch in the region of $\delta = 0$–0.3π.

Table 1. Frequencies and Assignments of IR Bands in the CH_2 Rocking Region

Estimated phase angles		Observed frequencies/cm^{-1}				
Oleic acid		Oleic acid		n-C_9H_{20}[a]	n-$C_{15}H_{32}$[a]	Assignments[b]
CH_3 side	CO_2 side	γ phase	α phase			
$\pi/14$		724	722		722	$R_1(CH_3$ side)
	$\pi/8$	727	727	727		$R_1(CO_2H$ side)
$3\pi/14$		730	729		722	$R_2(CH_3$ side)
	$2\pi/8$	730	729			$R_2(CO_2H$ side)
	$3\pi/8$	737	737	736		$R_3(CO_2H$ side)
$5\pi/14$		745			744	$R_3(CH_3$ side)
	$4\pi/8$	765	768	770		$R_4(CO_2H$ side)
$7\pi/14$		788			778	$R_4(CH_3$ side)
	$5\pi/8$	820	821	821		$R_5(CO_2H$ side)
$9\pi/14$		854	859		851	$R_5(CH_3$ side)

a) Data of Snyder and Schachtschneider.[33] b) R: ν_8 branch modes.

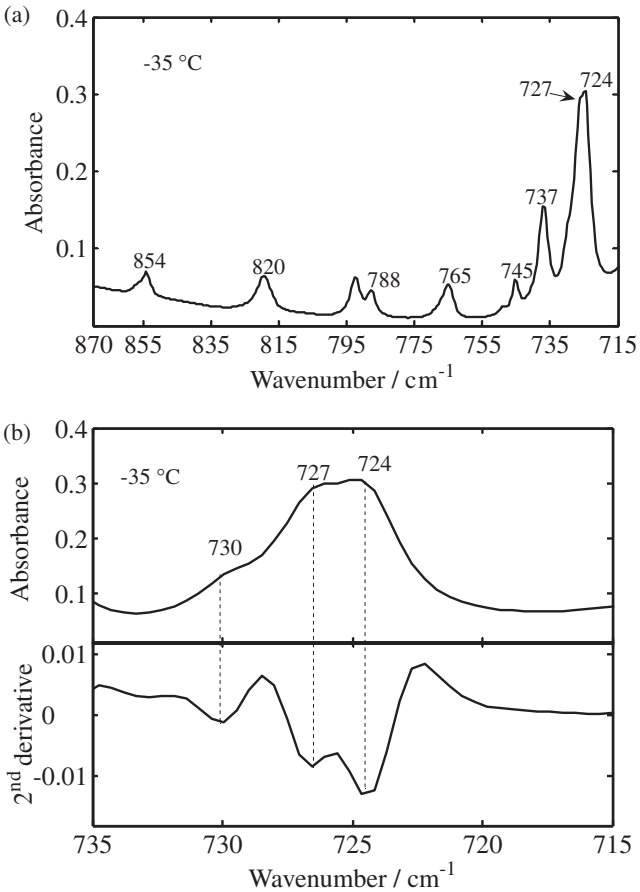

Figure 3. The progression bands (a) due to CH_2 rocking–CH_2 twisting modes in the γ phase, (b) an enlargement of band around 725 cm^{-1} (upper part) and corresponding second derivatives (bottom part).

As for n-alkanes having N pieces of CH_2 groups,[33] the ν_8 progression bands are characterized by δ_k given by:

$$\delta_k = k\pi/(N+1) \quad k = 1, 2, \ldots, N$$

On the basis of the estimated values for δ_k, it is expected that the progression bands of the carboxy-terminus chain appear close to those of n-C_9H_{20}, and the progression bands of the methyl-terminus chain appear close to those of n-$C_{15}H_{32}$. The observed frequencies of the progression bands in the γ phase are summarized in Table 1, in comparison with those in n-C_9H_{20} and n-$C_{15}H_{32}$.[33] The progression bands of the γ phase are actually observed at frequencies very close to the corresponding ones in n-C_9H_{20} and n-$C_{15}H_{32}$. Figure 4 shows the frequency vs. δ plot constructed with the data in Table 1. This plot well represents the features of the ν_8 branch. The results in Table 1 and Figure 4 suggest the validity of the assignments.

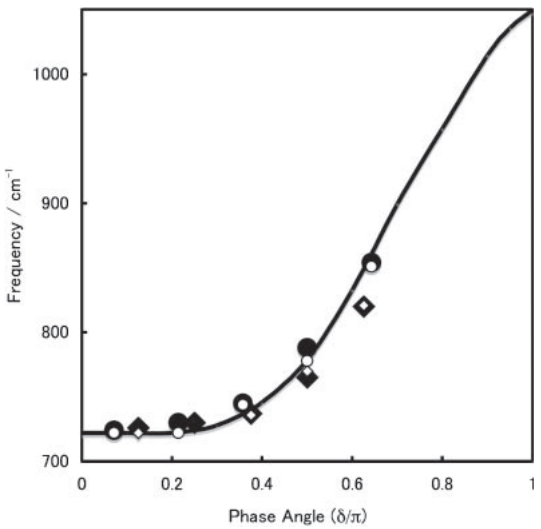

Figure 4. Frequency–phase angle relationship of the ν_8 branch modes and observed frequency data of the methyl-terminus chain (●) and carboxy-terminus chain (◆) in the γ phase of oleic acid and n-$C_{15}H_{32}$ (○) and n-C_9H_{20} (◇). The solid line represents the dispersion curve obtained with the data of Snyder and Schachtschneider.[33]

Spectral Changes from the γ to α Phase on a Heating Process. As shown in the overall spectra in Figure 2a, many IR bands exhibit drastic changes at the $\gamma \rightarrow \alpha$ phase-transition point. The detailed assignments of the characteristic bands due to the *cis*-olefin, methyl, and carboxy groups are summarized in Table 2. These bands show obvious changes in the $\gamma \rightarrow \alpha$ phase transition.

Table 2. IR Bands Associated with the Functional Groups in the γ and α Phases of Oleic Acid

Functional group	γ phase /cm^{-1}	α phase /cm^{-1}	Assignments
cis-Olefin group	2995	3002	=C–H stretching vibration
	1661	1655	C=C stretching vibration
	703	—	=C–H out-of-plane bending
Methyl group	2954	2954	Asymmetric C–H stretching (in-plane)
	2943	—	Asymmetric C–H stretching (out-of-plane)
	2869	2872	Symmetric C–H stretching
	1446	—	Asymmetric C–H bending
	1370	1380	Symmetric C–H bending
	893	895	CH_3–C rocking
Carboxy group	1687	1688	C=O stretching vibration
	925 921	919	O–H out-of-plane wagging
	688	689	O–C=O in-plane bending

First, remarkable spectral changes are observed particularly for the bands concerning the *cis*-olefin group, which generates an intense band assignable to =C–H out-of-plane bending, γ(=C–H), at 703 cm^{-1} in the γ phase (Figure 2b). The γ(=C–H) band is very sensitive to the conformation around the *cis*-olefin group. It remarkably collapses into the background (Figure 2b) accompanying the line broadening and large shifts from 2995 to 3002 cm^{-1} of the =C–H stretching, ν(=C–H), band after the $\gamma \rightarrow \alpha$ phase-transition point (Figure 2c). These intense variances at the phase-transition point incontrovertibly reflect the large conformational changes of the *cis*-olefin group from skew–*cis*–skew′ to skew–*cis*–*trans*.

Second, the bands due to the methyl group also show remarkable changes at the transition point. For example, the symmetric CH bending, $\delta_s(CH_3)$, band at 1370 cm^{-1} quickly shifts to 1380 cm^{-1} (Figure 5a), and the CH_3–C rocking, r(CH_3), band at 893 cm^{-1} smears (Figure 5b) after the transition point. In addition to these spectral variations at the transition point, the profile of the $\delta_s(CH_3)$ band changes continuously accompanied by a gradual intensity decrease and broadening of the r(CH_3) band in the γ phase as the temperature increases, as shown in Figures 5a and 5b.

Third, the temperature dependences of the bands due to the carboxy group are considerably different when compared with the bands due to the methyl and *cis*-olefin groups. Some discontinuities are also observed in the carboxy-group bands, but the frequency shifts (Table 2) and intensity changes at the phase-transition point are rather small (Figures 6 and 7) compared with the variances related to the methyl and *cis*-olefin groups. Even so, obvious spectral changes still take place in the γ phase as the temperature increases up to the transition point. For example, the C=O stretching, ν(C=O), band in the 1720–1665 cm^{-1} region shows a gradual intensity decrease and increase in the lower and higher frequency regions separated by an isosbestic point at 1690 cm^{-1} (Figure 6a). The O–H out-of-plane bending, σ(O–H), band exhibits a similar spectral change, i.e., a clear continuous intensity decrease and increase occur respectively in the higher and lower frequency regions separated by an isosbestic point at 917 cm^{-1} (Figure 6b). A characteristic spectral change in the γ phase is also observed around 1300 cm^{-1}, where the bands due to the CH_2 wagging modes coupled with the C–O stretching mode appear.[15,33] That is, the peak at 1299 cm^{-1} gradually increases in intensity as the temperature rising (Figure 6c).

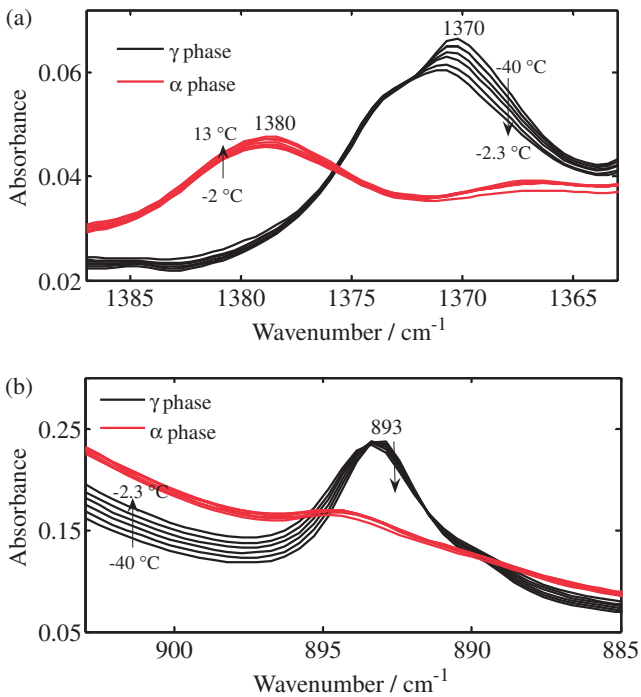

Figure 5. Spectral changes of the bands associated with the methyl group from −40 to 13 °C: (a) symmetric C–H bending band and (b) CH_3–C rocking band (↓: an intensity decrease with a temperature increase; ↑: an intensity increase with a temperature increase).

In the α phase, different types of continuous changes are observed in the carboxy bands. In the ν(C=O) region (Figure 7a), the portion around 1710 cm^{-1} swells out as the temperature rises with one overlapping peak at 1698 cm^{-1} after the $\gamma \rightarrow \alpha$ phase-transition point, in particular rapidly in the vicinity of the melting point. For the σ(O–H) band, it continuously decreases in intensity without isosbestic point following a sharp disappearance of the novel band in the γ phase at 925 cm^{-1} after the phase-transition point (Figure 7b).

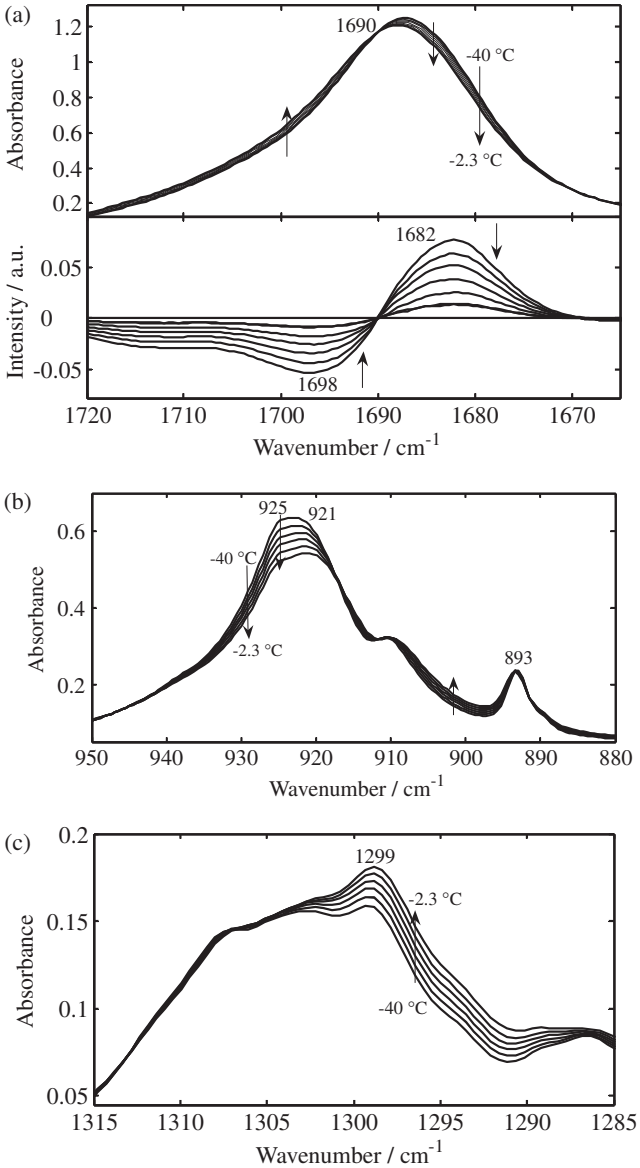

Figure 6. Spectral changes of the bands associated with the carboxy group in the γ phase from −40 to −2.3 °C: (a) the C=O stretching band in the region of 1720–1665 cm^{-1} (upper part) and corresponding difference spectra calculated with the spectrum at −2.3 °C as reference (bottom part), (b) the O–H out-of-plane band, and (c) the region of the CH_2 wagging modes (↓: intensity decrease with temperature increase; ↑: intensity increase with temperature increase).

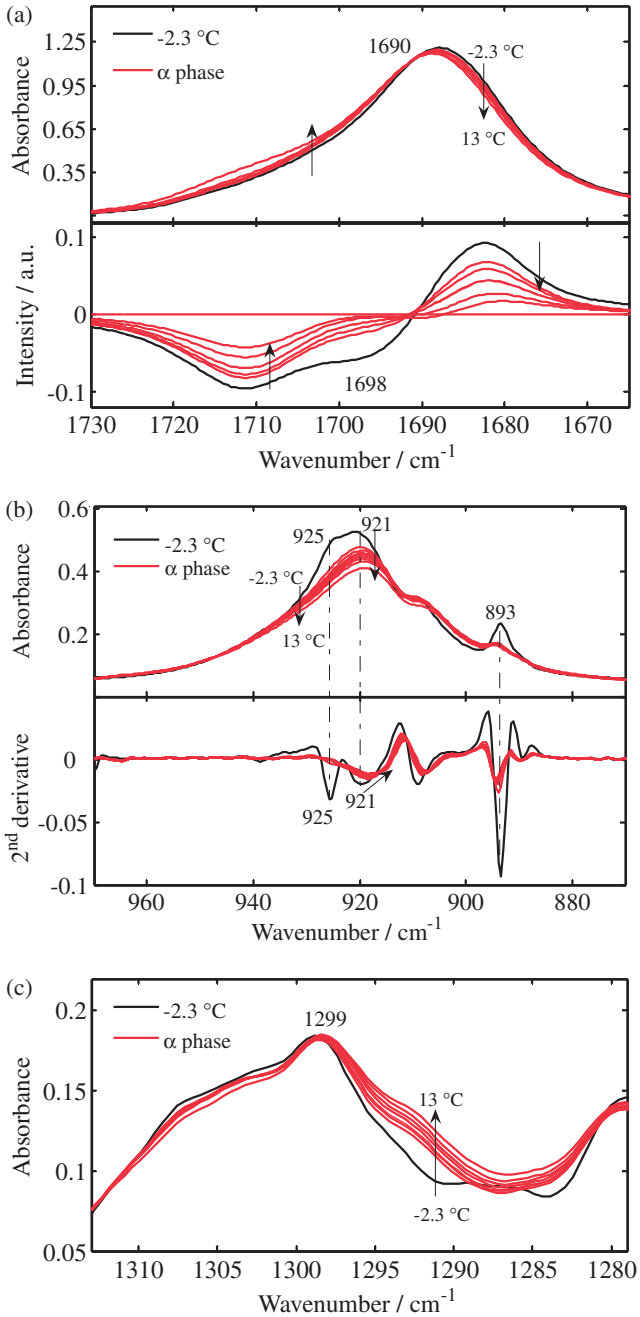

Figure 7. Spectral changes of the bands associated with carboxy group around the $\gamma \rightarrow \alpha$ transition point, −2.3 °C, and in the α phase from 0 to 13 °C: (a) the C=O stretching band (upper part) and corresponding difference spectra calculated with the spectrum at 13 °C as reference (bottom part), (b) the O–H out-of-plane band (upper part) and corresponding second derivatives (bottom part), and (c) the region of the C–O stretching mode coupled with the CH_2 wagging mode (↓: an intensity decrease with a temperature increase; ↑: an intensity increase with a temperature increase).

Nevertheless, the intensity increase of the peak at 1299 cm^{-1} no longer occurs, but a continuous intensity increase takes place in the low-frequency side of this peak (Figure 7c).

Discussion

Structural Changes on the $\gamma \rightarrow \alpha$ Phase Transition. The characteristics of the IR spectral changes observed in the γ and α phases in the present study can be summarized as follows:

(1) Many IR bands, in particular those which are associated with the portion from the *cis*-olefin group to the methyl group, show sudden and drastic changes at the $\gamma \rightarrow \alpha$ transition point. On the other hand, there are no essential spectral variations that indicate a definite structural change in the temperature region of the γ phase, except small spectral changes in the bands associated with the carboxy and methyl groups.

(2) The spectral changes at the transition point in the bands associated with the carboxy group are rather small, compared with those in the bands associated with the *cis*-olefin and methyl groups.

(3) As for the ν_8 progression bands, the bands due to the methyl-terminus chain exhibit larger spectral changes than those due to the carboxy-terminus chain in the γ phase. Moreover, at the $\gamma \rightarrow \alpha$ transition point, the bands associated with the methyl-terminus chain show abrupt changes compared with the bands attributed to the carboxy-terminus chain.

These facts indicate that the basic structural features of the γ phase, i.e., two ordered hydrocarbon chains linked to the *cis*-olefin group of skew–*cis*–skew′ conformation and accommodated in the $O'_{\parallel}$ subcell, remain unchanged until the transition point, and then oleic acid undergoes discontinuously structural changes primarily in the portion between *cis*-olefin group and methyl group. These results deduced from the present study are highly consistent with the results of previous solid-state NMR and Raman spectroscopic studies.[15,16,21,22] As derived from the temperature dependence of Raman spectra in oleic acid and erucic acid,[16,18,21] the sudden occurrence of conformational disordering in the methyl-terminus chain accompanying a large conformational transformation around *cis*-olefin group characterize the $\gamma \rightarrow \alpha$ transition.

Methyl Groups in the γ Phase. As illustrated in Figure 8, the band width of the $r(CH_3)$ band gradually increases with the intensity decreasing before the sudden variance at the phase-transition point, i.e., in the temperature region of the γ phase. Moreover, these changes in band width and intensity show a larger temperature dependence than those of the γ(=C–H) band in the temperature region of the γ phase. Nevertheless, the values of intensity and band width of the $r(CH_3)$ band remain constant compared with the continuous evolutions of the γ(=C–H) band in the α phase. According to previous Raman studies,[15,16] the conformational disordering at the vicinity of the methyl terminal does not start up to the transition point. The same result was also obtained by solid-state NMR study;[22] there is no clear upfield shift of the methyl carbon due to the *gauche*-conformation. Furthermore, drastic frequency shifts and profile changes only occur at the phase-transition point for all IR bands due to the methyl group. Thus, it is reasonable to deduce that the results obtained at the methyl terminal in the present study confirm the previous propositions determined from Raman spectral and solid-sate NMR measurements.

Generally the methyl terminal is the most mobile part of dimeric fatty acids in crystalline states. Moreover, according to our previous X-ray study on erucic acid,[18] the γ phase shows a significant anisotropy as to lattice expansion; although the thickness of the bimolecular layer remains almost constant until the transition point, the lattice expands solely in the lateral direction of acyl chains with temperature. A similar lattice expansion can be assumed to occur in the γ phase of oleic acid. Therefore, it is reasonable to relate the gradual changes of the $\delta_s(CH_3)$ and $r(CH_3)$ bands in the temperature region of the γ phase not to the conformational disordering but to an increase in the mobility of the methyl terminal. The continuous lattice expansion reduces the intermolecular interactions between the methyl terminals and increases the thermal fluctuation, which is considered to cause the gradual spectral changes of the methyl bands.

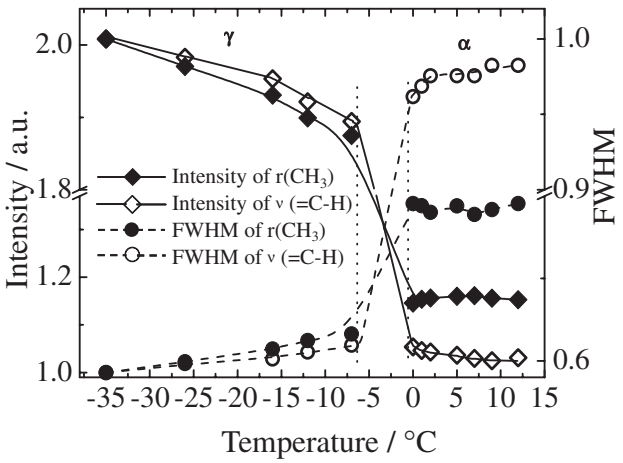

Figure 8. Temperature dependences of the intensity (solid line) and full width at half maximum (FWHM) (dash line) of the CH_3–C rocking, $r(CH_3)$, (◆) and the =C–H stretching vibration, ν(=C–H), (□) bands in the phase transition. The data are relative values compared with the intensity and FWHM at −40 °C.

Characteristics of the ν_8 Progression Bands. As summarized in Figure 9a and Table 1, the ν_8 progression bands exhibit characteristic spectral changes in the $\gamma \rightarrow \alpha$ phase transition. The shape of the 725 cm^{-1} band drastically changes, since the 724 cm^{-1} component due to the methyl-terminus chain becomes a shoulder at 722 cm^{-1}, while the 727 cm^{-1} component due to the carboxy-terminus chain remains almost unchanged. Although each progression band exhibits an intensity decrease and a frequency shift, there is a tendency that the frequency shifts of the methyl-terminus bands are larger than those of the carboxy-terminus bands. With respect to the temperature dependence of band width in the γ phase, there is a clear difference between the methyl-terminus bands and the carboxy-terminus bands with $k = 4$ and 5. To take an example of $k = 5$, the methyl-terminus band at 854 cm^{-1} shows a larger temperature dependence than the carboxy-terminus at 820 cm^{-1}, as shown in Figure 9b.

Not only the γ phase, but also the α phase exhibits a series of ν_8 progression bands with weaker intensities and wider band widths due to the methyl and carboxy-terminus chains. Since the progression bands are caused by hydrocarbon chains of ordered conformation, this suggests that the methyl-terminus chain takes an extended conformation at a high ratio in the α phase, which is consistent with the conclusion of the previous Raman study that only less than about 10% of the methyl terminals take disordered conformations except just under the melting point.[15,18]

As can be seen from Figure 4, the ν_8 branch is almost flat in the region of phase angles δ from 0 to 0.3π and changes very sharply in the region of 0.3π to π, which means that the sensitivity of the ν_8 branch mode to a phase-angle variation significantly depends on the location in the dispersion curve. Furthermore, the character of the ν_8 branch mode varies from pure CH_2 rocking, $r(CH_2)$, to pure CH_2 twisting, $t(CH_2)$, as the phase angle increases from 0 to π. Since the hydrogen atoms

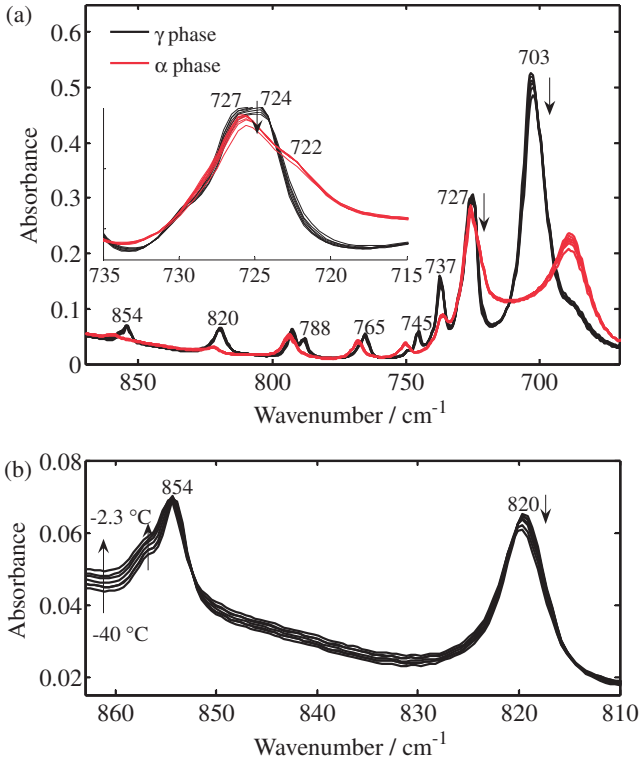

Figure 9. Spectral changes of the CH_2 rocking–CH_2 twisting progression bands: (a) the whole region from −40 to 13 °C, the γ and α phases, and (b) the bands with $k = 5$ from −40 to −2.3 °C (↓: an intensity decrease with a temperature increase; ↑: an intensity increase with a temperature increase).

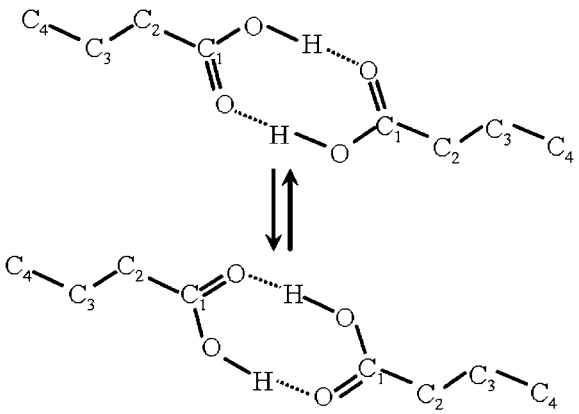

Figure 10. *cis* and *trans* Conformations of the dimerized carboxy group.

oscillate in the direction perpendicular to the chain axis, the r(CH_2) mode ($\delta \approx 0$) has a high susceptibility to the lateral packing of hydrocarbon chains. For example, the r(CH_2) band splits into a doublet at 720 and 730 cm^{-1} for the $O_\perp$ subcell. This susceptibility gradually declines as the t(CH_2) nature increases.[23,33] It follows that the influential factors in causing spectral changes in the ν_8 progression bands would vary depending on the phase angle.

The band due to the most-in-phase mode ($k = 1$) can be regarded as the r(CH_2) band, which is insensitive to a phase-angle variation and has a high sensitivity to the lateral packing of hydrocarbon chains. Based on the evolutions of the progression bands of methyl- and carboxy-terminus chains in the γ and α phases, it is reasonable to conclude that the subcell structure becomes looser for both the methyl- and carboxy-terminus chains but at different levels in the $\gamma \rightarrow \alpha$ transition. That is, the carboxy-terminus chain keeps the $O'_\parallel$ subcell in the whole transition, while the methyl-terminus chain rebuilds it into a looser subcell which brings higher mobility to the methyl terminal. Therefore, we may infer that the remarkable change of the 724 cm^{-1} band due to the methyl-terminus chain is attributable to the transformation of the subcell structure and the accompanying activation of molecular motion.

As plotted in Figure 4, the progression bands with $k = 3$ to 5 ($\delta > 0.35\pi$) become sensitive to a phase-angle variation. Therefore, in addition to lateral packing and molecular motion, other factors such as the boundary conditions and conformational order also bring about spectral changes in these modes. It can be considered that the boundary conditions are changed greater for the methyl-terminus chain than for the carboxy-terminus chain. Meanwhile, the packing of the methyl terminal becomes loose whereas that of the carboxy terminal remains almost unchanged in the $\gamma \rightarrow \alpha$ transition. It is because the dihedral angle of the C–C bond linked to the *cis*-C=C bond changes much more in the methyl terminus from the γ phase to the α phase. We infer that the larger change of the boundary conditions gives rise to a greater frequency shift to the progression bands due to the methyl-terminus chain. As shown in Figure 9b, the methyl-terminus bands with $k = 4$ and 5 exhibit a larger temperature dependence of band width than the carboxy-terminus ones in the γ phase. Since the methyl terminal becomes more mobile with temperature, it seems reasonable to attribute the larger temperature dependence of the methyl-terminus bands to the mobility increase of the methyl terminal.

So far, no detailed analysis has been carried out on the progression bands of oleic acid both by Raman and IR spectroscopy. However, the progression bands are easily observed by FTIR spectroscopy, moreover, we can use the enormous amount of information from previous IR studies on the progression bands of long-chain compounds, such as Snyder's work,[33] to analyze the spectrum of the molecular system we focus on. As described above, the progression bands observed in IR spectra can be used as a probe to sense the conditions of the methyl-terminus and the carboxy-terminus chains separately, just like the two intense Raman bands at 1125 and 1095 cm^{-1}, which are associated with the symmetric C–C stretching modes of the methyl and carboxy-terminus chains, respectively. We believe that a similar methodology can also be applied to systems containing unsaturated hydrocarbon segments based on the present study of the progression bands.

Structural Changes Associated with the Carboxy Group. Although some discontinuities are observed at the transition points (Figure 7), the alterations in the carboxy-group bands are on a small scale in comparison with the portions of *cis*-olefin group (Figures 2b and 2c) and methyl terminal (Figure 5). It is suggested that the carboxy group carries out a modest structure change at the transition point, which seems to be reasonable considering that the carboxy-terminus chain maintains the $O'_\parallel$ subcell in the whole phase transition process.

Besides the changes at the transition point, the ν(C=O) and σ(O–H) bands show continuous spectral changes with temperature in the γ phase (Figure 6). Judging from the extent of the spectral changes, it is thought that a minor localized structural variation takes place at the carboxy group. The isosbestic points found in the ν(C=O) and σ(O–H) bands suggest that the spectral change is probably caused by the displacement of an equilibrium between two different states of the carboxy group. Furthermore, the continuous intensity increase in the region around 1300 cm^{-1}, where the ν(C–O) mode is involved, also confirms that a certain structural change occurs at the carboxy group.

As described above, the unit cell expands solely in the lateral direction with temperature, which would change the intermolecular interactions exerted on the dimerized carboxy groups to induce some structural changes. Thus, it should be considered that the continuous structural change of the carboxy group in the γ phase is caused by an expansion of the unit cell.

An alternative candidate for the localized structural changes of carboxy groups is the *cis–trans* tautomerism, in which the location of the C=O and C–O bonds are exchanged by the transfer of hydrogen-bonded protons along hydrogen bonds in the dimerized carboxy groups (Figure 10).[34] Taking as an example even-numbered fatty acids, there are three polymorphs having the $O_\perp$ subcell, B, C, and E forms, all of which belong to a monoclinic system of space group $P2_1/a$.[35,36] The acyl chain inclines toward the a_s axis in the B and E forms and toward the b_s axis in the C form (here we take the subcell axes according to orthorhombic polyethylene determined by Bunn[37]). Although the acyl chain takes the all-*trans* conformation in the C and E forms, it bends at the C_2–C_3 bond in the B form. Among these polymorphs, only the C form shows the *cis–trans* tautomerism.[36] It is thought that the hydrogen-bonded O···O distance is closely related to the occurrence of *cis–trans* tautomerism. The O···O distance is 2.66 Å at −52 °C for the γ phase of erucic acid,[38] which is slightly shorter than the value found in the B and E forms at room temperature (2.68 and 2.67 Å). The hydrogen bonding is also reflected in the frequency of the σ(O–H) band; the peak of the σ(O–H) band is located at 945 cm^{-1} in the C form and at 895 cm^{-1} in the B and E forms.[27,36] In the γ phase, the peak falls at 923 cm^{-1}, about the midpoint between the two frequencies. These data suggest to some extent a possibility of the dynamic equilibrium between the *cis*- and *trans*-form of dimerized carboxy groups by the double proton transfer in the γ phase.

Also in the α phase, the carboxy bands exhibit continuous spectral changes but of somewhat different characteristics. For example, the intensity increase of the peak at 1299 cm^{-1} no longer takes place but the shoulder at 1293 cm^{-1} develops with temperature. It seems that the $\gamma \rightarrow \alpha$ transition makes the properties of carboxy group somewhat different. In the temperature region of the α phase, the lattice expansion in the lateral direction is continuing at a slightly larger rate.[18] In this circumstance, the intermolecular interactions exerted on carboxy groups decrease and the mobility of carboxy groups increases with temperature. The frequency of 1710 cm^{-1}, where a shoulder of the ν(C=O) band developing in the α phase, corresponds to that of the ν(C=O) band in molten oleic acid. We infer that a small ratio of carboxy groups begins to exist in a condition similar to the melt state in the temperature region close to the melting point.

As described above, the present IR experiments show that continuous structural alterations of the carboxy group, which are considered very difficult to detect by Raman spectroscopy, take place in the γ and α phases. However, there is a limit to the information obtained only from IR spectral data. Thus, with respect to the minute structure of the carboxy group and the more reliable and concrete model about the structural changes in the γ and α phases and at the $\gamma \rightarrow \alpha$ transition point, further detailed research including X-ray crystallography is necessary.

Conclusion

The structural evolutions and dynamic properties of oleic acid γ and α phases during heating have been followed by FTIR spectroscopy to shed some light on the different aspects of oleic acid from previous Raman studies. In addition to the bands associated with each functional group, the progression bands due to the CH_2 rocking–CH_2 twisting modes examined for obtaining information about the methyl-terminus and carboxy-terminus chains separately. The present study has confirmed that the abrupt structural changes in the $\gamma \rightarrow \alpha$ phase transition take place particularly in the portion from the *cis*-olefin group to the methyl terminal at the $\gamma \rightarrow \alpha$ phase-transition point. It is also shown that the molecular motion is activated more strongly at the methyl terminal in the γ phase. Moreover, this enhanced mobility at the methyl terminal in the γ phase operates as a predisordered stage of the abrupt structural evolutions at the phase-transition point (Figure 8).

The IR spectral data also indicate that the carboxy group carries out continuous structural changes in both the γ and α phases. It is suggested that there is an equilibrium shift between two different states of the carboxy group in the γ phase, and the carboxy group gradually begins to assume a character similar to that in the melt as the temperature approaches the melting point.

The present study demonstrates that the progression bands in IR spectra are usable as a probe for sensing the states of the methyl-terminus and carboxy-terminus chains separately. It is also shown that the susceptibility of FTIR spectroscopy to the terminal and polar-group modes is very effective in exploring the structural changes of *cis*-unsaturated fatty acids, in particular, in the detection of the structural changes of the methyl and carboxy groups.

References

1 J. M. Berg, J. L. Tymoczko, L. Stryer, *Biochemistry*, 6th ed., W. H. Freeman and Company, New York, **2007**.

2 D. Voet, J. G. Voet, *Biochemistry*, Wiley, New York, **1995**.

3 D. M. Samll, *The Physical Chemistry of Lipids: From Alkanes to Phospholipids*, Plenum Press, New York, **1986**.

4 B. L. Silver, *The Physical Chemistry of Membranes: An Introduction to the Structure and Dynamics of Biological Membranes*, Allen & Unwin, Boston, **1985**.

5 L. Stryer, *Biochemistry*, Freeman, New York, **1995**.

6 L. L. Pearce, S. C. Harvey, *Biophys. J.* **1993**, *65*, 1084.

7 L. Di, D. M. Small, *J. Lipid Res.* **1993**, *34*, 1611.

8 K. R. Applegate, J. A. Glomset, *J. Lipid Res.* **1991**, *32*, 1645.

9 S. C. Smolinske, *Handbook of Food, Drug, and Cosmetic Excipients*, CRC Press, Florida, **1992**.
10 R. G. Sinclair, A. F. Mckay, G. S. Mckay, R. N. Jones, *J. Am. Chem. Soc.* **1952**, *74*, 2578.
11 M. Suzuki, T. Ogaki, K. Sato, *J. Am. Oil Chem. Soc.* **1985**, *62*, 1600.
12 M. Kobayashi, in *Crystallization and Polymorphism of Fats and Fatty Acids*, ed. by N. Garti, K. Sato, Marcel Dekker, New York, **1988**.
13 S. Abrahamsson, I. Ryderstedt-Nahringbauer, *Acta Crystallogr.* **1962**, *15*, 1261.
14 F. Kaneko, K. Yamazaki, K. Kitagawa, T. Kikyo, M. Kobayashi, Y. Kitagawa, Y. Matsuura, K. Sato, M. Suzuki, *J. Phys. Chem. B* **1997**, *101*, 1803.
15 M. Kobayashi, F. Kaneko, K. Sato, M. Suzuki, *J. Phys. Chem.* **1986**, *90*, 6371.
16 Y. Kim, H. L. Strauss, R. G. Snyder, *J. Phys. Chem.* **1988**, *92*, 5080.
17 M. Suzuki, K. Sato, N. Yoshimoto, S. Tanaka, M. Kobayashi, *J. Am. Oil Chem. Soc.* **1988**, *65*, 1942.
18 F. Kaneko, K. Yamazaki, M. Kobayashi, Y. Kitagawa, Y. Matsuura, K. Sato, M. Suzuki, *J. Phys. Chem.* **1996**, *100*, 9138.
19 K. Sato, in *Advance in Applied Lipid Research*, ed. by F. B. Padley, JAI Press, New York, **1996**, Vol. 2.
20 F. Kaneko, K. Yamazaki, M. Kobayashi, K. Sato, M. Suzuki, *Spectrochim. Acta, Part A* **1994**, *50*, 1589.
21 P. Tandon, G. Förster, R. Neubert, S. Wartewig, *J. Mol. Struct.* **2000**, *524*, 201.
22 C. Akita, T. Kawaguchi, F. Kaneko, H. Yamamoto, M. Suzuki, *J. Phys. Chem. B* **2004**, *108*, 4862.
23 M. Tasumi, T. Shimanouchi, A. Watanabe, R. Goto, *Spectrochim. Acta* **1964**, *20*, 629.
24 R. G. Sinclair, A. F. McKay, R. Norman Jones, *J. Am. Chem. Soc.* **1952**, *74*, 2570.
25 R. Norman Jones, A. F. McKay, R. G. Sinclair, *J. Am. Chem. Soc.* **1952**, *74*, 2575.
26 R. F. Holland, J. Rud Niesen, *J. Mol. Spectrosc.* **1962**, *9*, 436.
27 I. Fischmeister, *Prog. Chem. Fats Other Lipids* **1975**, *14*, 91.
28 W. G. De Ruig, *Appl. Spectrosc.* **1977**, *31*, 122.
29 J. Yano, F. Kaneko, M. Kobayashi, K. Sato, *J. Phys. Chem. B* **1997**, *101*, 8112.
30 T. Ishioka, W. Yan, H. L. Strauss, R. G. Snyder, *Spectrochim. Acta, Part A* **2003**, *59*, 671.
31 M. Tasumi, T. Shimanouchi, T. Miyazawa, *J. Mol. Spectrosc.* **1962**, *9*, 261.
32 M. Tasumi, S. Krimm, *J. Chem. Phys.* **1967**, *46*, 755.
33 R. G. Snyder, J. H. Schachtschneider, *Spectrochim. Acta* **1963**, *19*, 85.
34 S. Hayashi, J. Umemura, *J. Phys. Chem.* **1975**, *63*, 1732.
35 G. Degerman, E. von Sydow, *Acta Chem. Scand.* **1959**, *13*, 984.
36 M. Kobayashi, F. Kaneko, *J. Dispersion Sci. Technol.* **1989**, *10*, 319.
37 C. W. Bunn, *Trans. Faraday Soc.* **1939**, *35*, 482.
38 F. Kaneko, K. Yamazaki, M. Kobayashi, Y. Kitagawa, Y. Matsuura, K. Sato, M. Suzuki, *Acta Crystallogr., Sect. C* **1993**, *49*, 1232.